A Finite Element Analysis Model for Internal Partial Discharges in an Air-Filled, Cylindrical Cavity inside Solid Dielectric

Moein Borghei
ECE Department
Virginia Tech
Blacksburg, VA, USA

Mona Ghassemi
ECE Department
Virginia Tech
Blacksburg, VA, USA

Behzad Kordi
ECE Department
University of Manitoba
Winnipeg, MB, Canada

Puneet Gill
ECE Department
University of Manitoba
Winnipeg, MB, Canada

Derek Oliver
ECE Department
University of Manitoba
Winnipeg, MB, Canada

***Abstract*—The reliability of electrical equipment is closely tied with the health of their insulation system. A well-known symptom of the aging phenomenon in dielectrics is partial discharge (PD) which can occur in all media. Internal PDs in solid dielectrics occur in air-filled voids which are difficult to eliminate thoroughly and may appear simply during the manufacturing process. Although much research on PD measurement for solid dielectrics has been conducted, this is not the case for PD modeling. Besides, the simulation of a case study and its comparison with experimental results can provide further insights into the possibility of other PD sources. In this paper, a finite element analysis (FEA) model for internal PD in an air-filled cylindrical void inside a solid dielectric under 60 Hz sinusoidal voltage is developed. For the estimation of the parameters of the model, experimental data is needed. To this end, a cylindrical void was artificially made within a 3D-printed polylactic acid (PLA) block. Then, phase-resolved partial discharge (PRPD) patterns were measured for the mentioned samples. Using deterministic PD measurement data, an FEA model was developed. This model will help us understand and explain internal PD behavior for the case of a cylindrical void and study the influence of void size on PD behavior.**

Keywords— ***Finite element analysis, insulation systems, internal partial discharges, polylactic acid (PLA).***

I. Introduction

The insulation system is an inseparable part of electrical equipment and its reliable operation keeps the conductive parts electrically apart. The failure of the insulation system can lead to a short-circuit and cause the failure of the entire equipment. Therefore, it is crucial to identify, model, and mitigate the insulation aging mechanisms.

One of the most important aging factors in dielectric materials is partial discharges (PDs). This phenomenon can occur in any medium (i.e., gases, liquids, and solids) and it also has three types: internal discharges, surface discharges, and corona. While PDs do not cause an abrupt breakdown of dielectric material, they can accelerate the deterioration rate of the material's insulating properties and reduce the equipment's life expectancy [1].

The PD crisis is an important design factor in almost any electrical equipment including electric motors, power electronics converters, more electric aircraft, etc. [2-8]. In solid dielectrics, the material often contains cavities or voids within the dielectric material or on the boundaries between the insulating material and the electrodes. These voids are usually contemplated as weak points due to their susceptibility to PDs. The weakness arises from the fact that the dielectric constant of an air-filled cavity is lower than the surrounding material and the electric field in this region can go higher than its proximity.

There are several models proposed in the literature for internal discharge modelings such as the three-capacitance model [9], induced-charge model [10, 11], plasma dynamics model [12], and finite-element analysis (FEA) model [13-16]. In this paper, FEA is used as it is capable of handling sophisticated geometries efficiently as well as its ability to dynamically monitor changes in the values of electrical properties such as electric field, current density, and field displacement [17-22].

The objective of this study is to develop an FEA model based on experimental data aiming to provide further insights into the PD mechanism and other potential sources of PD besides internal discharges. The experimental results and the model are based on the 3D printed cylindrical block of Polylactic Acid (PLA) as the dielectric which has an artificial cylindrical void at its center.

In Section II, the experimental setup is introduced. In Section III, the FEA model and the algorithm details are discussed. The results are demonstrated and analyzed in section IV. In the end, Section V gives conclusions.

II. Experimental Setup

To assess the performance of the proposed modeling scheme to reproduce real PD results, a 3D-printed cylindrical PLA was used which had a cylindrical void at its center. The experiment setup and calibration follow the IEC 60270 standard and are shown in Figure 1.

To reduce the imperfections that existed in the sample, the settings of the 3D printer are adjusted. Also, the sample is 3 mm in height and 12 mm in diameter. The control sample showed no PD under an applied voltage of 10 kV.

The high voltage and ground electrodes are brass cylinders with a diameter of 10 mm. The entire sample and electrodes were immersed in transformer oil to prevent surface discharges (see Figure 2).

2021 IEEE Electrical Insulation Conference (EIC) | 978-1-6654-1564-4/21/$31.00 ©2021 IEEE | DOI: 10.1109/EIC49891.2021.9612268

Fig. 1. Experimental setup.

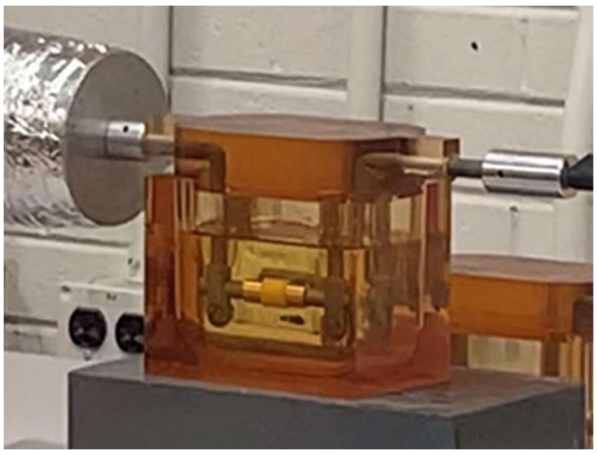

Fig. 2. Sample between the electrodes immersed in transformer oil.

III. FEA Model

To simulate the dielectric-void configuration numerically, the finite element method (FEM) is used to estimate the electric field distribution in the domain and compare the outcome with the experimental results. Since the partial discharge phenomenon is strongly dependent upon electric field distribution, an accurate estimation of the electric field distribution leads to an accurate and effective investigation of PD activities. The reproduction of the experimental results is based upon the assumption that the PD activities all stemmed from the cylindrical void (the interference of imperfections and impurities is neglected).

The inception of a PD event is controlled by two factors: (1) the presence of at least one free electron, and (2) the electric field that is high enough to energize the free electron(s) and give rise to further ionization. The first factor is a stochastic phenomenon. To compare the simulation results with the experimental results, we assume that the provision of the initial electron occurs at the same time as the experimental case.

The rest of the process of the PD simulation is shown in Figure 3. The algorithm starts with the import of PD data. In this study, the dataset includes the PD apparent charge and extinction time/phase. Then, the PD events are sequentially reproduced as follows: the first PD event is different from the rest of the discharges as it provides a normalizing index for the next events. For the reproduction of any PD event, one quantity is fixed (it is determined by the measurement data): PD extinction time. However, there are two degrees of freedom provided by PD inception time and maximum cavity conductivity. The measurements do not provide the magnitude of these quantities, but the PD charge magnitude is affected by these parameters. Therefore, for each discharge, we have a list of inception times, $\boldsymbol{T_{inc}^{list}}$, and a list of maximum cavity conductivities, $\boldsymbol{\sigma_{c,m}^{list}}$. The FEA model is run for each combination of inception time, t_{inc}^{j}, and maximum conductivity, $\sigma_{c,m}^{k}$ and the corresponding apparent charge magnitude is stored as q_{jk}^{i}. In the case of the first discharge, we find the combination (j^*, k^*) that is the closest to the measured apparent charge. The ratio of the simulated and actual charge magnitudes (δ) is then defined which will be used as a calibration factor for the next discharges. For any FEA model, the process starts with the update of time profile such that the time-stepping occurs more gently during the PD transient state that has a duration in the scale of nanoseconds.

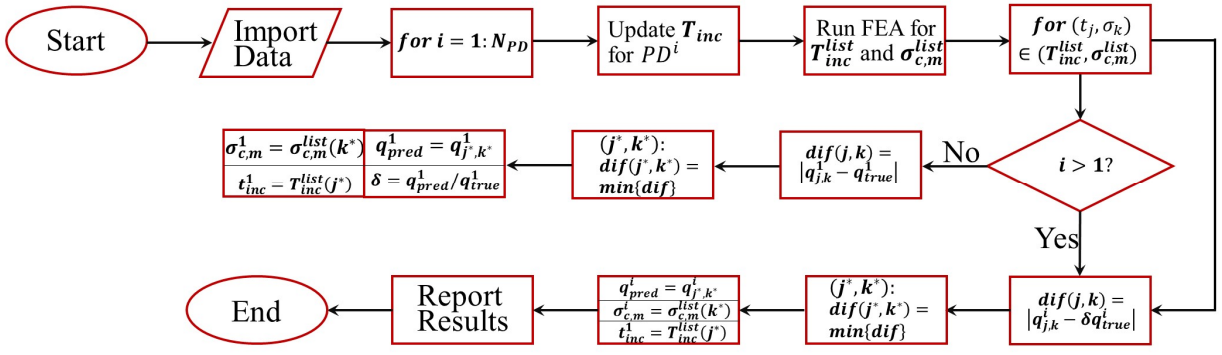

Fig. 3. The algorithm for reproduction of PD results

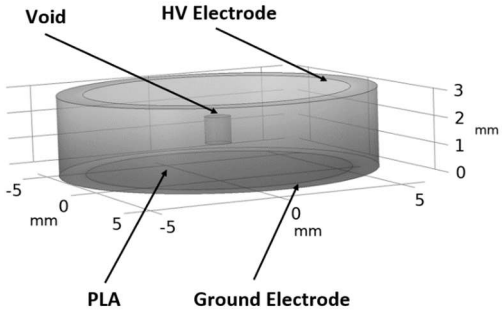

Fig. 4. Simulation geometry

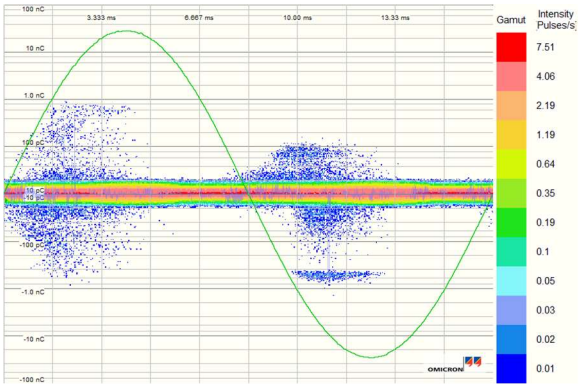

Fig. 5. Phase-resolved PD Pattern (PRPD) for a void size of 1mm

Thereafter, the cavity conductivity is updated to capture the change in the state of the cavity from non-conductive to conductive ($\sigma_{c,m}^{i}$) during the discharge. This FEA model can run in COMSOL Multiphysics® to find the electric field distribution across the cavity-insulation domain.

For the next PD events, the process is almost the same; the only difference is that the charge factor, δ, is used to compare the simulated charged magnitude with the actual charge magnitude. This process is continued until covering all the discharges. The entire algorithm is implemented in MATLAB® which is interfaced with COMSOL Multiphysics®.

IV. Results

The 3D geometry of the void-dielectric system is shown in Figure 4. Due to the symmetry of the configuration, we use the 2D axisymmetric representation of geometry that reduces the computational burden considerably.

The experiments are performed based on IEC 60270 for the PLA sample when a 60-Hz voltage is applied to the HV electrode. Figure 5 shows the PRPD pattern for this sample. The sample without artificial void does not present any PD for the voltages below 10 kV. In the case of a sample with 1-mm void, the discharges start to appear at a voltage level of 4.6 kV. The reproduced PDs in this study are based on the measurement performed at $V_{rms} = 4.6\ kV$.

For the test sample, we apply Algorithm 1 to capture the first 10 discharges ($N_{PD} = 10$). The time-step during the transient state is $1\ ns$. The extinction electric fields for the

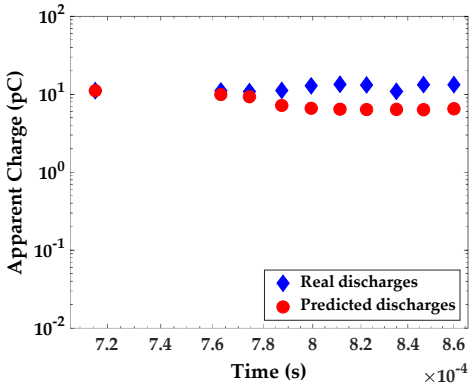

Fig. 6. The distribution of first 10 discharges over time for the void size of 1 mm.

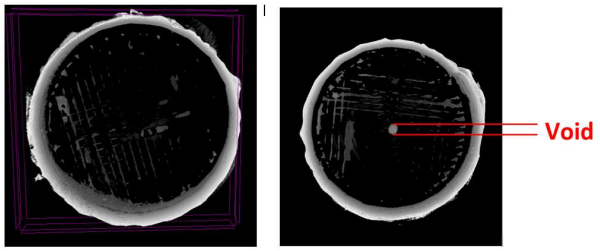

Fig. 7. μCT image of sample with (a) no void, and (b) 1 mm void.

discharges are determined by the measurements (which are based on the phase of the voltage at the extinction time). The dielectric constant and conductivity of PLA considered for the model are 3.1 and 10^{-14} S/m, respectively [23].

The list of the candidates for maximum cavity conductivity includes 5 values: 0.00005, 0.0001, 0.0005, 0.001, and 0.005 all in S/m. Also, the list of discharge durations, based on which the $\boldsymbol{T_{inc}^{list}}$ is defined, includes durations of 3000, 2000, 1000, and 500 ns. Note that the optimal choice of t_{inc} and $\sigma_{c,m}$ is made through a spline interpolation using all the combinations of the above values.

The results of the FEA model, in comparison with experimental results, are shown in Figure 6. At the first glance, the similar trend of discharges over time and the closeness of magnitudes of discharges look salient. The former could be expected as the provision of the initial free electron for the PD events was calibrated with the experimental results. Also, the latter indicates the robust performance of the algorithm in the reproduction of the results. An accurate reproduction of the measurement results through only two degrees of freedom (PD duration and cavity conductivity) introduces a great potential to model discharges based on the correct adjustment of the two parameters mentioned above.

However, it is noteworthy to mention that after the first couple of discharges, a small gap ($1\ pC - 6.5\ pC$) appears between the measured and simulated charge magnitudes. This

observation demonstrates the existence of other PD sources that act in tandem with the artificial cylindrical void.

This is also logical since the simulation considers an ideal dielectric, but in the real world, there are still microscopic defects in the body and at the surface of the dielectric.

To investigate this further, X-ray images of PLA samples were acquired using a Bruker Sky-scan 1275 micro-CT instrument (Fig. 7). X-ray images confirm the presence of unwanted voids inside the samples albeit very few and small. The control sample (i.e. the sample with no intentional void) shows imperfections that appear in form of air gaps/voids especially in the periphery of the dielectric(Fig. 7a). It appears that the imperfections were formed along the path of movement of the printer nozzle. Fig. 7b shows the sample with a 1-mm void. The same horizontal imperfections/defects are again visible.

V. Conclusions

The proliferation of electrical equipment and the escalated tension on insulation systems due to new generations of power electronic modules urges the accurate analysis and modeling of the partial discharge phenomenon. In this study, PD tests and simulation methods are integrated to investigate the internal partial discharge activities in an artificial, cylindrical void in the 3D-printed PLA stressed by the HV system. The experimental results detect PD activities for a cavity-dielectric test system including a 1-mm (height and diameter) cylindrical void. The reproduced PD events are generally in agreement with the measured. The charge magnitude of the discharges after the initial discharges, however, shows a small degree of discrepancy which is a potential sign of other unwanted PD sources such as printing imperfections inside the insulation block and surface discharges. The X-ray images of the PLA block confirm the existence of such impurities. Future studies will focus on producing 3D-printed samples with higher precision in which the interference of natural voids is negligible compared to the artificial voids.

Acknowledgment

This work was supported in part by the Air Force Office of Scientific Research under Award FA9550-20-1-033, in part by the Office of Naval Research (ONR) under Award N00014-19-1-2343, and in part by the National Science Foundation (NSF) under Award 1942540.

References

[1] B. Zhang, M. Ghassemi, and Y. Zhang, "Insulation materials and systems for power electronics modules: A review identifying challenges and future research needs," *IEEE Trans. Dielectr. Electr. Insul.*, vol. 28, no. 1, pp. 290–302, Feb. 2021.

[2] M. Ghassemi, "Accelerated insulation aging due to fast, repetitive voltages: A review identifying challenges and future research needs," *IEEE Trans. Dielectr. Electr. Insul.,* vol. 26, no. 5, pp. 1558–1568, Oct. 2019.

[3] M. Ghassemi, "PD measurements, failure analysis, and control in high-power IGBT modules," *High Voltage*, vol. 3, no. 3, pp. 170–178, Sep. 2018.

[4] N. D. Jacob, D. R. Oliver, S. S. Sherif, and B. Kordi, "Statistical texture analysis of morphological changes in pressboard insulation due to thermal aging and partial discharges," *IEEE Electr. Insul. Conf. (EIC)*, Seattle, WA, USA, 2015, pp. 610–613.

[5] A. N. Esfahani, S. Shahabi, G. Stone, and B. Kordi, "Investigation of corona partial discharge characteristics under variable frequency and air pressure," *IEEE Electr. Insul. Conf. (EIC)*, San Antonio, TX, USA, 2018, pp. 31–34.

[6] M. Ghassemi, "Electrical insulation weaknesses in wide bandgap devices," in *Simulation and Modelling of Electrical Insulation Weaknesses in Electrical Equipment*, R. Albarracin Ed., London, U.K.: IntechOpen, 2018, pp. 129–149.

[7] A. Barzkar and M. Ghassemi, "Electric power systems in more and all electric aircraft: A review," *IEEE Access*, vol. 8, pp. 169314–169332, 2020.

[8] M. Borghei and M. Ghassemi, "Insulation materials and systems for more and all-electric aircraft: A review identifying challenges and future research needs," *IEEE Trans. Transport. Electrific.*, doi: 10.1109/TTE.2021.3050269.

[9] S. Whitehead, *Dielectric Breakdown in Solids*, Clarendon Press, 1951.

[10] G. C. Crichton, P. W. Karlsson, and A. Pedersen, "Partial discharges in ellipsoidal and spheroidal voids," *IEEE Trans. Dielectr. Electr. Insul*., vol. 24, no. 2, pp. 335–342, Apr. 1989.

[11] A. Pedersen, G. C. Crichton, and I. W. McAllister, "The theory and measurement of partial discharge transients," *IEEE Trans. Dielectr. Electr. Insul*., vol. 26, no. 3, pp. 487–497, Jun. 1991.

[12] G. Callender, T. Tanmaneeprasert, and P. L. Lewin, "Simulating partial discharge activity in a cylindrical void using a model of plasma dynamics," *J. Phys. D: Appl. Phys*., vol. 52, no. 5, 2019.

[13] C. Forssen and H. Edin, "Partial discharges in a cavity at variable applied frequency part 2: measurements and modeling," *IEEE Trans. Dielectr. Electr. Insul.,* vol. 15, no. 6, pp. 1610–1616, 2008.

[14] H. Illias, G. Chen, and P. L. Lewin, "Partial discharge behavior within a spherical cavity in a solid dielectric material as a function of frequency and amplitude of the applied voltage," *IEEE Trans. Dielectr. Electr. Insul.*, vol. 18, no. 2, pp. 432–443, Apr. 2011.

[15] M. Borghei, M. Ghassemi, J. M. Rodríguez-Serna, and R. Albarracín Sánchez, "A finite element analysis and an improved induced charge concept for partial discharge modeling," *IEEE Trans. Power Del.*, 2020, Early Access. DOI: 10.1109/TPWRD.2020.2991589

[16] M. Borghei and M. Ghassemi, "Finite element modeling of partial discharge activity within a spherical cavity in a solid dielectric material under fast, repetitive voltage pulses," *IEEE Electr. Insul. Conf. (EIC)*, Calgary, Canada, 2019, pp. 34–37.

[17] M. Borghei and M. Ghassemi, "Partial discharge finite element analysis under fast, repetitive voltage pulses," *IEEE Electric Ship Technologies Symposium (ESTS)*, Arlington, VA, USA, 2019, pp. 324–328.

[18] M. Borghei and M. Ghassemi, "Partial discharge analysis under high-frequency, fast-rise square wave voltages in silicone gel: A modeling approach," *Energies*, vol. 12, no. 23, p. 4543, Nov. 2019.

[19] M. Borghei and M. Ghassemi, "Characterization of partial discharge activities in WBG power modules under low-pressure condition," *IEEE Conf. Electr. Insul. and Dielectr. Phenom. (CEIDP)*, East Rutherford, NJ, USA, 2020, pp. 297-300.

[20] M. Borghei and M. Ghassemi, "A finite element analysis model for partial discharges in silicone gel under a high slew rate, high-frequency square wave voltage in low-pressure conditions," *Energies*, vol. 13, no. 9, p. 2152, May 2020.

[21] M. Borghei and M. Ghassemi, "Effects of low–pressure condition on partial discharges in WBG power electronics modules*," IEEE Electr. Insul. Conf. (EIC)*, Knoxville, TN, USA, 2020, pp. 199–202.

[22] M. Borghei and M. Ghassemi, "Investigation of low-pressure condition impact on partial discharge in micro-voids using finite-element analysis," *IEEE Energy Conversion Cong. Expo. (ECCE)*, Detroit, MI, USA, 2020, pp. 3293–3298.

[23] C. Dichtl, P. Sippel, and S. Krohns, "Dielectric Properties of 3D Printed Polylactic Acid," *Advances in Materials Science and Engineering*, vol. 2017, p. 6913835, Jul. 2017.